

A two-band tight-binding model of spin-polarized transport in magnetic tunnel junctions

N. Strelokov¹, M. Zhuravlev^{2,3*}, N. Ryzhanova¹, A. Vedyayev¹

¹Department of Physics, Lomonosov Moscow State University, Moscow, Russia

²Kurnakov Institute of General and Inorganic Chemistry of RAS, Moscow

³Smolny College of Liberal Arts and Sciences, St. Petersburg State University, St. Petersburg, Russia

Email address:

nik@magn.ru (N. Strelokov), myezhur@gmail.com (M. Zhuravlev)

To cite this article:

N. Strelokov, M. Zhuravlev, N. Ryzhanova, A. Vedyayev. A two-band tight-binding model of spin-polarized transport in magnetic tunnel junctions, *International Journal of Materials Science and Applications*. Vol. 2, No. 1, 2013, pp. 20-29. doi: 10.11648/j.ijmsa.20130201.13

Abstract: The main features determining spin-dependent transport in magnetic tunnel junctions are well appreciated now mainly due to ab initio calculations. Nevertheless, it seems useful to have a comparatively simple model which reproduces the salient characteristics of spin-dependent transport in magnetic multilayers. We present two-band tight-binding model of magnetic tunnel junction with the layers of arbitrary thickness and non-collinear magnetization configuration. The model accounts for different symmetry of the tunneling electrons and their mixing on the interfaces. As an illustration for double-barrier structure we calculate I-V curves and spin-transfer torque. The calculations demonstrate the resonant character of the I-V dependences. Also, the significant difference in the magnitude of the torque acting on the various planes of the same magnetic layer is found.

Keywords: Magnetic Tunnel Junction, Two-Band Model, I-V Curves, Spin-Transfer Torque

1. Introduction

For the last twenty years, the intensive investigation of giant magnetoresistance (GMR) in magnetic multilayers and tunneling magnetoresistance (TMR) in magnetic tunnel junctions (MTJ) has offered a rather comprehensive view of these phenomena. Various methods and models were proposed to treat spin-dependent transport in magnetic multilayers. Semiclassical approaches based on Boltzmann equation account for spin-dependent scattering in the bulk of magnetic layer via spin-dependent mean free path [1, 2]. Quantum theories of spin-dependent transport in magnetic multilayers [3-6] take into account the quantization of electron momentum and the scattering on the potential barriers between successive layers. These theories give the description of ballistic as well as diffusive spin-dependent transport in magnetic multilayers. Among the quantum models of spin-dependent transport in the multilayers, the free-electron as well as tight-binding models were used. Model calculations [7, 8] predicted huge increase of TMR in double (and more) barrier structure due to resonant tunneling. The fitting of first principle calculation of band parameters was used to get quantitative description of specific systems.

The first-principle calculations of spin-dependent trans-

port in magnetic tunnel junctions [9-11] revealed the details of TMR and GMR mechanisms in ballistic regime. It was shown in [11] that in ballistic regime TMR is determined by the coupling of Bloch states of different symmetries with the evanescent states in the barrier layers which have the slowest decay. In particular, it was shown that huge TMR value in Fe(100)/MgO/Fe(100) three-layer is due to transmission through $\Delta 1$ states in parallel configuration which are s-like in majority channel whereas in antiparallel configuration the conductance is very low, since mainly d-like $\Delta 1$, $\Delta 2'$, and $\Delta 5$ states give the main contribution into current. Spin-dependent transmission was calculated for different structures distinguished by the number of the atomic layers. The role of interfacial hybridization between the electron states of different symmetries was clarified due to this investigation. Later the influence of s-d hybridization on TMR for MgO-based magnetic tunnel junctions was investigated in two-band free electron model [12]. The description of various theoretical approaches to spin-dependent tunneling in MTJ can be found in [13].

Another important factor affecting GMR and TMR is the electron structure of the interfaces. The significant role of the interfaces was made clear by model and first-principle calculations [11, 14]. The influence of the bonding on the

adjacent layers on the transmission of the spin channels increases as the barrier thickness decreases. The role of interfaces in spin-dependent transport was investigated for different MTJ, for instance, Fe/MgO, Co/Al₂O₃ interfaces were considered in [14, 15].

Still another aspect of spin-dependent transport in multilayers is the current induced magnetization switching in magnetic multilayers due to spin-transfer torque [16] acting on the magnetization of the magnetic layer. It originates from spin angular moment transfer between the conducting electrons and the magnetization of the layer [17-21] in non-collinear MTJ. This subject attracts much attention due to its technological application in memory devices. The critical current (the lowest current amplitude which produces the magnetization switching) is an important characteristics, and sometimes it is crucial for functionality of a device. The search for heterostructures with low critical current (including the heterostructures in which comparatively low current produces comparatively high torque) is an important task of applied studies.

Though the cited works together with other investigations in this field give general description of GMR and TMR, a simple tight-binding model which retains the essential features of the spin-dependent tunneling in real materials still seems important and useful. In the present work we develop tight-binding model which takes into account the conducting electrons of two different symmetries and their hybridization on the interfaces. Our model accounts for hybridization of the electrons of different symmetries on the interfaces. We can vary the number and the thickness of the layers and the mutual orientation of the magnetization of magnetic layers. By choosing relative band parameters we can make the contribution of the electrons of specific symmetry dominant in majority or minority channel. As an illustration we calculate I-V curves and the torque for five-layer system for various magnetic configurations of the systems.

2. Model

2.1. Selecting a Template (SciencePG-Level2-single-line)

Our tight-binding model retains the following features of spin-dependent tunneling in MTJ. We consider two kinds of electron states which correspond to the Bloch states of two different symmetries. The transmission is determined by the coupling of these states in ferromagnetic conducting layers with the evanescent states in barrier layers. As an example we can take the electron structure of Fe/MgO/FeMTJ, where Δ_1 states which demonstrate the slowest decay in the barrier are in majority channel whereas in the minority channel the electrons of other types of symmetry are presented [11]. We refer to these electrons with different orbital symmetry as “s-electrons” and “d-electrons”. Both bands are exchange-split in the ferromagnetic layers. To take into account the difference between interfacial hoppings of the electrons and the hoppings inside a layer, we separate these two parts explicitly:

$$\hat{H} = \sum_N \hat{H}_N^L + \sum_M \hat{H}_M^I \quad (1)$$

where the first summation is taken over the index of the layers and the second is taken over the interfaces. In (1) operator \hat{H}_N^L is the Hamiltonian of the L th layer (which can be ferromagnetic as well as insulating). The Hamiltonian of N th ferromagnetic layer has the following form:

$$\begin{aligned} \hat{H}_N^L = \sum_{\langle nm \rangle, \sigma} \{ & t_{s\uparrow\uparrow}^F(n, m) s_n^{\uparrow+} s_m^{\uparrow+} + t_{s\downarrow\downarrow}^F(n, m) s_n^{\downarrow+} s_m^{\downarrow+} + \\ & t_{d\uparrow\uparrow}^F(n, m) d_n^{\uparrow+} d_m^{\uparrow+} + t_{d\downarrow\downarrow}^F(n, m) d_n^{\downarrow+} d_m^{\downarrow+} \\ & + \sum_{n, \sigma} \epsilon_s^{0\sigma} s_n^{\sigma+} s_n^{\sigma-} + \epsilon_d^{0\sigma} d_n^{\sigma+} d_n^{\sigma-} \} \end{aligned} \quad (2)$$

In (2)

$$s_m^{\sigma-}, s_m^{\sigma+}, d_m^{\sigma-}, d_m^{\sigma+}$$

are the annihilation and creation operators of s- or d-electrons on site m. The parameters

$$\epsilon_s^{0\sigma}, \epsilon_d^{0\sigma}$$

determine the position of the corresponding band

$$\sigma = \uparrow \text{ or } \downarrow$$

is spin projection index. The summation in (2) is taken over the sites and the pairs of the nearest sites which are located in the same layer. The functional form of the Hamiltonian is identical for ferromagnetic and for barrier layers. In the case of a barrier the index “F” has to be replaced by index “B”. It is clear from (2) that we describe the barrier by rectangular potential.

We emphasized in (2) that hopping integrals depend on the sites. To simplify the problem we divide the hopping term of Hamiltonian (2) into two parts. The first one contains the hopping between the sites of the same plane. We denote this summation by the sign “ \parallel ”. The second part contains the hopping perpendicular to the plane and, therefore the sites belong to the neighboring planes. We denote this summation by the symbol “ \perp ” (To avoid misunderstanding we note that we use the terms “layer” and “plane” for different objects, namely, in our consideration a layer consists of several planes).

$$\begin{aligned} \hat{H}_N^L = \sum_{\langle nm \rangle} \parallel \{ & -\eta_s^{\uparrow} s_n^{\uparrow+} s_m^{\uparrow+} - \eta_s^{\downarrow} s_n^{\downarrow+} s_m^{\downarrow+} - \eta_d^{\uparrow} d_n^{\uparrow+} d_m^{\uparrow+} - \eta_d^{\downarrow} d_n^{\downarrow+} d_m^{\downarrow+} \} + \\ \sum_{\langle nm \rangle} \perp \{ & -(t_s^F + \Delta t_s^F) s_n^{\uparrow+} s_m^{\uparrow+} - (t_s^F - \Delta t_s^F) s_n^{\downarrow+} s_m^{\downarrow+} - \\ & (t_d^F + \Delta t_d^F) d_n^{\uparrow+} d_m^{\uparrow+} - (t_d^F - \Delta t_d^F) d_n^{\downarrow+} d_m^{\downarrow+} \} \end{aligned}$$

$$+ \sum_{n,\sigma} \left\{ \varepsilon_s^{0\sigma} s_n^{\sigma+} s_n^{\sigma} + \varepsilon_d^{0\sigma} d_n^{\sigma+} d_n^{\sigma} \right\} \quad (3)$$

We assume the identical transversal hoppings for both types of electrons. This assumption allows us to reduce the problem to effective one-dimensional problem. Corresponding transversal hopping integrals are denoted in (3) by

$$\eta_{s,d}^{\sigma}$$

The terms

$$\Delta t_{s(d)}^F$$

take into account the difference in the hopping integrals for spin-up- and spin-down- electrons.

Each interfacial Hamiltonian deals with a pair of the neighboring sites, $n, n+1$, and can be divided into four parts. In the formula of interfacial Hamiltonian presented below, we drop the index “M” which numerates the interfaces.

$$\hat{H}^I = \hat{H}_{ss}^I + \hat{H}_{dd}^I + \hat{H}_{sd}^I + \hat{H}_{ds}^I = \sum_{a,b=s,d} \hat{H}_{ab}^I \quad (4)$$

Each term in (4) has the same angle dependence. This dependence originates from non-collinearity of the magnetization of different magnetic layers. The difference is only in the magnitude of coefficients. In contrast with Hamiltonian of a layer, the interlayer Hamiltonian contains only the hoppings perpendicular to the planes. The hoppings within a layer are included in

$$\hat{H}_N^L$$

If one of the neighboring layers is ferromagnetic, the interlayer Hamiltonian depends on the angle

$$\theta$$

which is the magnetization direction of the magnetic layer in a global coordinate frame. We assume that magnetization vector is directed parallel to the planes.

$$\begin{aligned} \hat{H}_{ab}^I = & -(t_{ab} + \Delta t_{ab}) \cos(\theta/2) A_n^{\uparrow+} B_{n+1}^{\uparrow} \\ & -(t_{ab}^* + \Delta t_{ab}^*) \cos(\theta/2) B_{n+1}^{\uparrow+} A_n^{\uparrow} \\ & -(t_{ab} - \Delta t_{ab}) \cos(\theta/2) A_n^{\downarrow+} B_{n+1}^{\downarrow} \\ & -(t_{ab}^* - \Delta t_{ab}^*) \cos(\theta/2) B_{n+1}^{\downarrow+} A_n^{\downarrow} + \\ & -(\gamma_{ab} + \Delta \gamma_{ab}) \sin(\theta/2) A_n^{\uparrow+} B_{n+1}^{\downarrow} \\ & -(\gamma_{ab}^* + \Delta \gamma_{ab}^*) \sin(\theta/2) B_{n+1}^{\downarrow+} A_n^{\uparrow} \\ & -(\nu_{ab} - \Delta \nu_{ab}) \sin(\theta/2) A_n^{\downarrow+} B_{n+1}^{\uparrow} \\ & -(\nu_{ab}^* - \Delta \nu_{ab}^*) \sin(\theta/2) B_{n+1}^{\uparrow+} A_n^{\downarrow} \end{aligned} \quad (5)$$

The operators A, B are the s or d operators, according to the values of the indices a, b . Hamiltonian (5) includes the orbital mixing on the interfaces. Corresponding hopping integrals are denoted through

$$\gamma_{ab}, \nu_{ab}$$

symbols,

$$\Delta \gamma_{ab}, \Delta \nu_{ab}$$

reflect the difference in the hopping integrals for spin-up- and spin-down- electrons.

Now we can search for the wave function in the mixed

$$(k_x, k_y, z)$$

representation as

$$\begin{aligned} \tilde{\Psi}(x, y, l) = & \Psi_{\parallel}^s \cdot \Psi^s(k_x, k_y, z) s_{k_x, k_y, z}^{\sigma+} |0\rangle + \\ & \Psi_{\parallel}^d \cdot \Psi^d(p_x, p_y, z) d_{p_x, p_y, z}^{\sigma+} |0\rangle \end{aligned} \quad (6)$$

where

$$\begin{aligned} \Psi_{\parallel}^s = & \exp[ik_x a_{\parallel} x + ik_y a_{\parallel} y], \\ \Psi_{\parallel}^d = & \exp[ip_x a_{\parallel} x + ip_y a_{\parallel} y] \end{aligned} \quad (7)$$

and creation operators

$$s_{k_x, k_y, z}^{\sigma+}, d_{k_x, k_y, z}^{\sigma+}$$

create s - or d - electron with spin projection σ on the plane z with in-plane momentum k_x, k_y .

The factors $\Psi_{\parallel}^{s,d}$ of the wave function are effected only by “ \parallel ” summation in (3). Substituting (6), (7) into (1-3) we get an effective one-dimensional Hamiltonian with the renormalized on-site energies $\varepsilon_{s,d}^{0\sigma}$. This renormalization is due to the contribution from the in-plane motion

$$\begin{aligned} \varepsilon_s^{\sigma} = & \varepsilon_s^{0\sigma} - 2\eta_s^{\sigma} (\cos(k_x a_{\parallel}) + \cos(k_y a_{\parallel})), \\ \varepsilon_d^{\sigma} = & \varepsilon_d^{0\sigma} - 2\eta_d^{\sigma} (\cos(k_x a_{\parallel}) + \cos(k_y a_{\parallel})) \end{aligned} \quad (8)$$

As a result, we get one-dimensional problem for the function

$$\Psi_{\perp}^{s,d}(k_x, k_y, z) \quad (7)$$

This function is a wave function of one-dimensional effective Hamiltonian

$$\hat{H} = \sum_N \hat{H}_N^L + \sum_M \hat{H}_M^I \quad (9)$$

where

$$\begin{aligned} \hat{H}_N^L = & \sum_{\langle nm \rangle} -(t_s^F + \Delta t_s^F) s_n^{\uparrow+} s_m^{\uparrow} - (t_s^F - \Delta t_s^F) s_n^{\downarrow+} s_m^{\downarrow} - \\ & (t_d^F + \Delta t_d^F) d_n^{\uparrow+} d_m^{\uparrow} - (t_d^F - \Delta t_d^F) d_n^{\downarrow+} d_m^{\downarrow} \end{aligned}$$

$$+ \sum_{n,\sigma} \varepsilon_s^\sigma s_n^{\sigma+} s_n^\sigma + \varepsilon_d^\sigma d_n^{\sigma+} d_n^\sigma \quad (10)$$

In (10) the indices n, m are the numbers of the layers.

3. Construction of Wave Function

Now we construct the wave function Ψ . We search for the wave function in the form:

$$\Psi = \sum_i \left(f^\uparrow(l) s_i^{\uparrow+} |0\rangle + f^\downarrow(l) s_i^{\downarrow+} |0\rangle \right) + \left(g^\uparrow(l) d_i^{\uparrow+} |0\rangle + g^\downarrow(l) d_i^{\downarrow+} |0\rangle \right) \quad (11)$$

In (11) l is the number of a plane. We start with the solution of Schrödinger equation inside a layer

$$\hat{H} \frac{L}{N} \Psi = E \Psi \quad (12)$$

There is no mixing of different orbital states or different spin projections inside a layer, therefore, the equations for s- and d- electrons can be solved separately. Equation (12) is an equation for the functions

$$f^\sigma(l), g^\sigma(l)$$

As an example we write the equation for s-electrons with “up” spin projection in ferromagnetic layer. The action of the Hamiltonian on the wave function transforms the later in the following way:

$$\left\{ \sum_{n,\delta=\pm 1} -(t_s^F + \Delta t_s^F) s_n^{\uparrow+} s_{n+\delta}^\uparrow + \sum_m \varepsilon_s^\uparrow s_n^{\uparrow+} s_n^\uparrow \right\} \sum_l f^\uparrow(l) s_l^{\uparrow+} |0\rangle = \sum_{l,\delta=\pm 1} -(t_s^F + \Delta t_s^F) s_l^{\uparrow+} f^\uparrow(l + \delta) |0\rangle + \sum_l \varepsilon_s^\uparrow s_l^{\uparrow+} f^\uparrow(l) |0\rangle \quad (13)$$

Therefore, we get the equation for the function $f^\uparrow(l)$:

$$\sum_{\delta=\pm 1} -(t_s^F + \Delta t_s^F) f^\uparrow(l + \delta) + \varepsilon_s^\uparrow f^\uparrow(l) = E f^\uparrow(l) \quad (14)$$

Similarly to spin-up component of wave function we obtain:

$$\sum_{\delta=\pm 1} -(t_s^F - \Delta t_s^F) f^\downarrow(l + \delta) + \varepsilon_s^\downarrow f^\downarrow(l) = E f^\downarrow(l) \quad (15)$$

$$\sum_{\delta=\pm 1} -(t_d^F + \Delta t_d^F) g^\uparrow(l + \delta) + \varepsilon_d^\uparrow g^\uparrow(l) = E g^\uparrow(l) \quad (16)$$

$$\sum_{\delta=\pm 1} -(t_d^F - \Delta t_d^F) g^\downarrow(l + \delta) + \varepsilon_d^\downarrow g^\downarrow(l) = E g^\downarrow(l) \quad (17)$$

where E is the energy of the state.

The solutions of these equations are known:

$$f^\uparrow(l) = A_F^\uparrow \exp[ik_{FM}^\uparrow al] + B_F^\uparrow \exp[-ik_{FM}^\uparrow al] \quad (18)$$

$$-2(t_s^F + \Delta t_s^F) \cos(k_{FM}^\uparrow a) + \varepsilon_{s,F}^\uparrow = E \quad (19)$$

$$f^\downarrow(l) = A_F^\downarrow \exp[ik_{FM}^\downarrow al] + B_F^\downarrow \exp[-ik_{FM}^\downarrow al] \quad (20)$$

$$-2(t_s^F - \Delta t_s^F) \cos(k_{FM}^\downarrow a) + \varepsilon_{s,F}^\downarrow = E \quad (21)$$

$$g^\uparrow(l) = C_F^\uparrow \exp[ip_{FM}^\uparrow al] + D_F^\uparrow \exp[-ip_{FM}^\uparrow al] \quad (22)$$

$$-2(t_d^F + \Delta t_d^F) \cos(p_{FM}^\uparrow a) + \varepsilon_{d,F}^\uparrow = E \quad (23)$$

$$g^\downarrow(l) = C_F^\downarrow \exp[ip_{FM}^\downarrow al] + D_F^\downarrow \exp[-ip_{FM}^\downarrow al] \quad (24)$$

$$-2(t_d^F - \Delta t_d^F) \cos(p_{FM}^\downarrow a) + \varepsilon_{d,F}^\downarrow = E \quad (25)$$

The equations (19), (21), (23), (25) determine the corresponding wave numbers. We use the notations $k_{FM}^{\uparrow,\downarrow}$ and $p_{FM}^{\uparrow,\downarrow}$ for z — components of s- and d- electrons respectively. We use index “F” to mark the values corresponding to ferromagnetic layer everywhere, except for the wave number for which we use index “FM” not to mistake it with Fermi momentum. The index “B” refers to the barrier layers. All symbols in (18) – (25) must have one additional index which is the index of the layer. We drop this index to make the expressions less cumbersome. The equations (19), (21), (23), (25) are written for a ferromagnetic layer, similar equations can be written for the barriers.

The coefficients

$$A_F^\sigma(B), B_F^\sigma(B), C_F^\sigma(B), D_F^\sigma(B)$$

are different in different layers. Schrödinger equation provides for the relation between the coefficients in the neighboring layers. This is the usual transfer matrix approach [22]. Some details of the calculation are placed in the Appendix.

The above form of the wave function is correct for the rectangular potential, i.e. in the case of vanishingly small voltage, when the linear response approximation can be applied. We deal with finite voltage across the system, since we calculate I-V curves. Therefore, we must add some additional potential $V(l)$ to each plane. We consider ballistic

conductivity, so the finite voltage drop takes place in the barrier segments. Assuming linear drop of the voltage across the barrier layers, one can express the exact wave function in the barriers through Airy functions. To simplify the calculations we used WKB approximation (for the system with the barriers see, for instance, [23]). The same transfer-matrix scheme is applied in this case as well.

4. Calculation of I-V Curves and Torque

Though we cannot describe real systems as accurately as it is done in ab initio approaches, we can reproduce the essential features of band structure of magnetic multilayers. As an example we present the calculations for the parameters which retain the main features of Fe/MgO heterostructure. We consider double-barrier structure which includes two outer ferromagnetic layers (electrodes) and two barriers separated by ferromagnetic layer. Each of the three interior layers consists of three planes.

To get the correct wave function decay in the barrier obtained from the first-principle calculations, we choose the following parameters.

In ferromagnetic layer,

$$a = 2.87 \text{ \AA} -$$

lattice parameter;

$$t_{s,F} = 0.363 \text{ eV} - s-s$$

hopping integral;

$$t_{d,F} = 0.340 \text{ eV} - d-d$$

hopping integral;

$$\Delta t_s = 0 -$$

the difference in “up” and “down” hoppings for s-electrons;

$$\Delta t_d = 0 -$$

the difference in “up” and “down” hoppings for d-electrons;

$$\varepsilon_{s,F}^{\uparrow} = 0, \quad \varepsilon_{s,F}^{\downarrow} = 4.359 -$$

the center of spin-up and spin-down s-bands in the ferromagnetic layers;

$$\varepsilon_{d,F}^{\uparrow} = -6.612, \quad \varepsilon_{d,F}^{\downarrow} = -2.540 -$$

the center of spin-up and spin-down d-bands in the ferromagnetic layers;

$$k_{s,F}^F = 0.97, \quad k_{d,F}^F = 0.32 -$$

Fermi momentum in the ferromagnetic layers.

In barrier layers we adopt

$$t_{s,B} = t_{d,B} = 1.22 \text{ eV}; \quad \varepsilon_{s,B} = 8.213 \quad \varepsilon_{d,B} = -37.856 -$$

the center of s- d-bands in the barrier layers;

$$k_{s,B}^F = 0.387, \quad k_{d,B}^F = 1.14 -$$

Fermi momentum in the ferromagnetic layers;

$$t_{sd}^{\uparrow,\downarrow} = t_{ds}^{\uparrow,\downarrow} = \sqrt{t_{s,F} t_{d,F}} -$$

interfacial hopping which mixes the orbitals.

These parameters allow us to get the correct density of states in the layers. The densities of states are shown on Fig. 1. This Figure demonstrates the main features which determine spin-dependent electron transport in the multilayer. Specifically, in the ferromagnetic layers only s-up and d-down subbands are conducting. The conductance of multilayer is strongly influenced by the interfacial mixing of the orbitals and the mutual orientation of the magnetization of the magnetic layers.

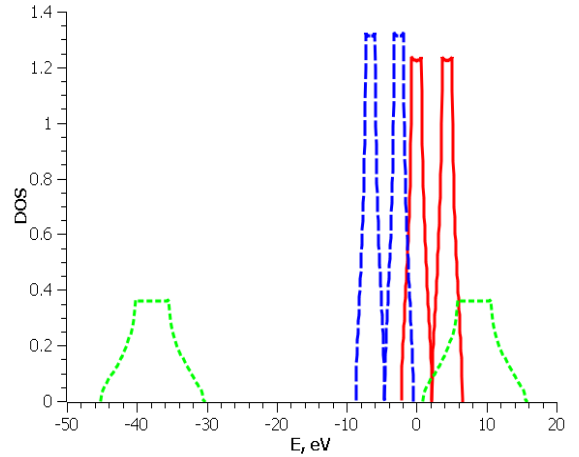


Figure 1. The density of states (DOS) of spin-up and spin-downs- and d-subbands in the ferromagnetic and the barrier layers. DOS of s-subbands in the ferromagnets are shown by solid lines, DOS of d- of states of spin-up subbands are shown by dashed lines, DOS of s- and d-subbands in the barrier are shown by dotted lines.

Landauer formula [24] for the current for the present case can be written as

$$I^\sigma = \frac{e}{\hbar} \frac{1}{(2\pi)^3} \frac{t_{s(d)}^{(n)}}{t_{s(d)}^{(1)}}$$

$$\int \frac{|\sin k_{s(d)}^{\sigma(n)} a| |\psi_{s(d)}^{\sigma*} \psi_{s(d)}^{\sigma}|}{|\sin k_{s(d)}^{\sigma(1)} a|}$$

$$[f^{(1)}(\epsilon) - f^{(n)}(\epsilon)]d\epsilon dk_x dk_y \quad (26)$$

In (26) we suppose that the coefficient of the incoming wave is chosen to be equal to the unity (in the left layer

$A_F^\sigma = C_F^\sigma = 1$) the upper index “(1)” refers to the first layer, the upper index “(n)” refers to the right outer layer where only the transmitted wave is present. As an illustration, we performed the calculations of I-V curves for five-layer systems, each layer (magnetic or non-magnetic) consists of three planes. The Figs. 2-4 display the I-V curves. Since s- and d- electrons are hybridized, we can not separate the two contributions. Instead, we calculated I-V curves for the waves obeying different boundary conditions, namely, for s-up and d-down waves coming from the left. We will call these states s- and d- waves respectively.

Fig. 2 displays I-V curves for parallel configuration of five-layer system, where the magnetization of intermediate layer is opposite to the magnetization of the outer ferromagnetic layers. Contribution of s-wave is much higher than that of d-wave.

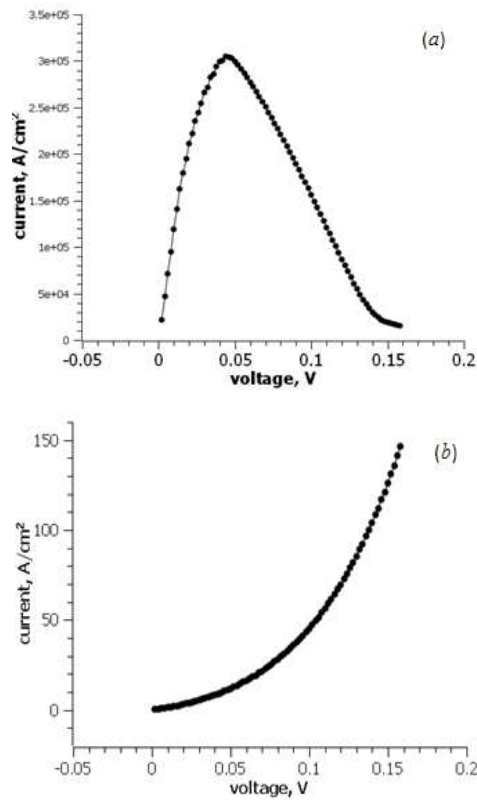


Figure 2. I-V curves for s- (a) and d- (b) waves and parallel configuration of five-layer system.

Fig. 3 represents I-V curves for antiparallel configuration (the magnetization of the right electrode is antiparallel to the magnetization of the left electrode and the magnetization of the middle ferromagnetic layer). It shows that conductance of d-electrons (Fig. 3b) can be high if the applied voltage provides for the resonant conductance of the corresponding subbands.

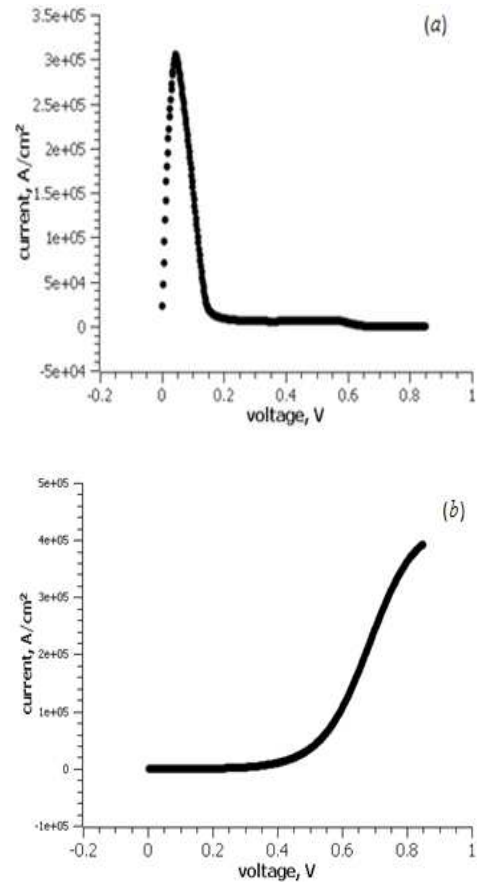
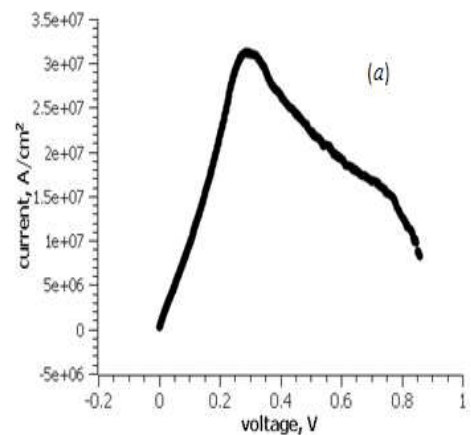


Figure 3. I-V curves for antiparallel configuration for s- (a) and d- (b) waves.

We also calculated I-V curve for mutual perpendicular orientation of the magnetizations (Fig. 4). By “perpendicular orientation” we mean the magnetic configuration of the multilayer when the magnetizations of left electrode and middle ferromagnet are parallel, whereas the magnetization of the right electrode is perpendicular to them. For such perpendicular orientation of the magnetizations of the layers and chosen parameters the contribution of d-electron is negligibly low.



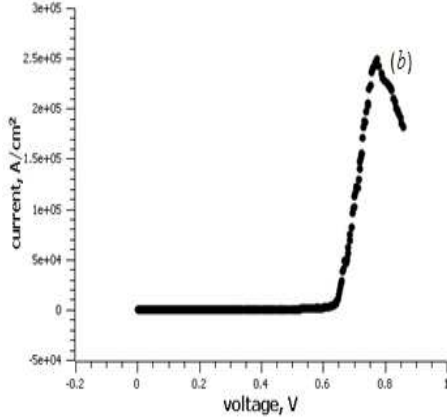


Figure 4. *I-V* curves for antiparallel configuration for *s*- (a) and *d*- (b) waves and perpendicular configuration.

Double-barrier structures are a common example of the possibility of resonant tunneling in multilayers. Figs. 2-4 clearly demonstrate the resonant conductance for some voltage. The drop of the current as the voltage increases is caused by the shift of the conducting bands. Moreover, due to resonant conductance the main contribution into current can originate from the electrons of different symmetries as the applied voltage increases.

Also, we have estimated the torque which acts on the magnetization of ferromagnetic plane from the spin-polarized current. We note that in the structure with the chosen band structure there are mainly *s*-electrons which produce the torque acting mainly on *d*-electrons of the magnetic layers. Following the model calculations developed in [25], we used the following expressions to estimate the torque:

$$T = \frac{J_{sd}}{\mu} \frac{a_1^2}{(2\pi)^3} \int \frac{\psi_s^\uparrow \psi_s^\downarrow}{2t_s \left| \sin k_s \frac{\uparrow(\downarrow)}{a_1} \right|} d\varepsilon dk_x dk_y \quad (27)$$

Wave function ψ_s^σ in (27) depends on the plane and the torque can be different for various planes in the same layer.

For perpendicular configuration of the magnetization, Fig. 5 displays the torque, which acts on various planes of the right ferromagnetic layer, as the function of the applied voltage. The torque drastically changes from plane to plane. Only the torque as the function of the voltage on the interfacial ferromagnetic layer (Fig. 5a) resembles corresponding *I-V* curve (Fig. 4). This difference in the torque magnitude for various planes is due to the evanescent states. The evanescent states do not contribute into the current, whereas these states contribute into the torque. Whereas current conserves, the torque demonstrates considerable variation from plane to plane as we see from Fig. 5. Also, we found that the torque changes its sign as the voltage increases, at least for some planes. Similar behavior of the torque dependence on

voltage was obtained in [26] by means of first principle calculations.

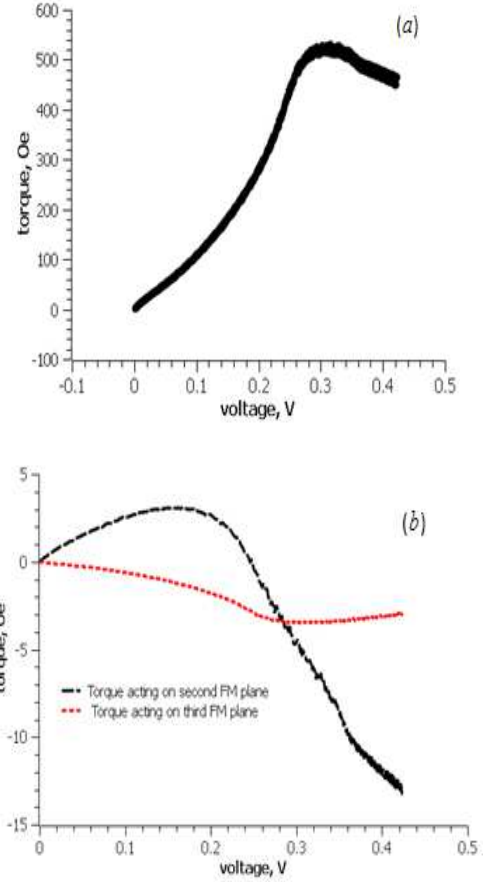


Figure 5. Torque acting on different planes of the ferromagnetic layer for perpendicular configuration. Fig. 5a represents the torque acting on the interfacial plane of the right ferromagnetic layer. Fig. 5b represents the torque acting on the two next layers (the “second” and the “third” planes in the right ferromagnetic layer).

5. Conclusion

In conclusion, we present a comparatively simple tight-binding model of multilayered system which takes into account two types of conducting electrons in the multilayer. These two types of electrons can refer to the electron states of different symmetry in real materials (like Δ_1 and Δ_5 in MgO). The thickness of the layers as well as the magnetization direction of the ferromagnetic layers can be chosen arbitrarily. By proper choice of the mutual position of these two exchange-splitting bands and the hybridization parameter t_{sd} we can reproduce essential features of spin-dependent transport in specific MTJ. The presented model can be used for the estimation of *I-V* curves and for the search for conductance and torque resonances in magnetic multilayers with large number of the layers and with various magnetic configurations. As an illustration, we calculated *I-V* curves and torque for some reasonable parameters and various mutual orientation of the layers magnetization in double MTJ. We found resonant behavior of the

current as a function of applied voltage. Also, we demonstrated that for certain orientation of the layers magnetization the torque drastically changes from plane to plane inside the same layer. For some layers the torque changes its sign as the function of the voltage. The model can be used for the calculation of some other characteristics of MTJs tightly related to transport properties, like interlayer exchange coupling [27].

Appendix

It is convenient to search for the wave function in the form (22), (24), (26), (28) for the inner plane of the layers. The values of the wave functions on the interfacial layers are used to construct the transfer matrix for the coefficients

$$A_{F(B)}^{\sigma}, B_{F(B)}^{\sigma}, C_{F(B)}^{\sigma}, D_{F(B)}^{\sigma}.$$

Let site M belong to ferromagnetic layer whereas site $M+1$ belong to the barrier. s -part of the Hamiltonian acts on the S component of the wave function as follows:

$$\begin{aligned} \hat{H}_{ss}^1 \Psi_s \equiv & \{ -(t_{ss} + \Delta t_{ss}) \cos(\theta/2) s_M^{\uparrow+} s_{M+1}^{\uparrow+} \\ & -(t_{ss}^* + \Delta t_{ss}^*) \cos(\theta/2) s_{M+1}^{\uparrow+} s_M^{\uparrow+} \\ & -(t_{ss} - \Delta t_{ss}) \cos(\theta/2) s_M^{\downarrow+} s_{M+1}^{\downarrow+} \\ & -(t_{ss}^* - \Delta t_{ss}^*) \cos(\theta/2) s_{M+1}^{\downarrow+} s_M^{\downarrow+} \\ & -(\gamma_{ss} + \Delta \gamma_{ss}) e^{-i\theta} \sin(\theta/2) s_M^{\uparrow+} s_{M+1}^{\downarrow+} \\ & -(\gamma_{ss}^* + \Delta \gamma_{ss}^*) e^{i\theta} \sin(\theta/2) s_{M+1}^{\downarrow+} s_M^{\uparrow+} \\ & -(v_{ss} - \Delta v_{ss}) e^{i\theta} \sin(\theta/2) s_M^{\downarrow+} s_{M+1}^{\uparrow+} \\ & -(v_{ss}^* - \Delta v_{ss}^*) e^{-i\theta} \sin(\theta/2) s_{M+1}^{\uparrow+} s_M^{\downarrow+} \\ & + \sum_{\sigma} \epsilon_{s,F}^{\sigma} s_M^{\sigma+} s_M^{\sigma} \\ & + \epsilon_{s,B}^{\sigma} s_{M+1}^{\sigma+} s_{M+1}^{\sigma} \} \sum_i (f^{\uparrow}(1) s_i^{\uparrow+} |0\rangle + f^{\downarrow}(1) s_i^{\downarrow+} |0\rangle) \quad (A1) \\ & -(t_{ss} + \Delta t_{ss}) \cos(\theta/2) s_M^{\uparrow+} f^{\uparrow}(M+1) |0\rangle \\ & -(t_{ss}^* + \Delta t_{ss}^*) \cos(\theta/2) s_{M+1}^{\uparrow+} f^{\uparrow}(M) |0\rangle \\ & -(t_{ss} - \Delta t_{ss}) \cos(\theta/2) s_M^{\downarrow+} f^{\downarrow}(M+1) |0\rangle \\ & -(t_{ss}^* - \Delta t_{ss}^*) \cos(\theta/2) s_{M+1}^{\downarrow+} f^{\downarrow}(M) |0\rangle \\ & -(\gamma_{ss} + \Delta \gamma_{ss}) \sin(\theta/2) s_M^{\uparrow+} f^{\downarrow}(M+1) |0\rangle \\ & -(\gamma_{ss}^* + \Delta \gamma_{ss}^*) \sin(\theta/2) s_{M+1}^{\downarrow+} f^{\uparrow}(M) |0\rangle \\ & -(\gamma_{ss} - \Delta \gamma_{ss}) \sin(\theta/2) s_M^{\downarrow+} f^{\uparrow}(M+1) |0\rangle \\ & -(\gamma_{ss}^* - \Delta \gamma_{ss}^*) \sin(\theta/2) s_{M+1}^{\uparrow+} f^{\downarrow}(M) |0\rangle \\ & + \sum_{\sigma} \epsilon_{s,F}^{\sigma} s_m^{\sigma+} f^{\sigma}(M) |0\rangle + \sum_{\sigma} \epsilon_{s,B}^{\sigma} s_{M+1}^{\sigma+} f^{\sigma}(M+1) |0\rangle \end{aligned}$$

Eq. (A1) includes

$$s_M^{\sigma+} |0\rangle$$

as well as

$$s_{M+1}^{\sigma+} |0\rangle$$

These terms relate to different layers. The same is true for d - wave functions. For the basis in the site

$$M \left(s_M^{\uparrow+} |0\rangle, s_M^{\downarrow+} |0\rangle, d_M^{\uparrow+} |0\rangle, d_M^{\downarrow+} |0\rangle \right)$$

we use the following Hamiltonian:

$$\begin{aligned} \hat{H}[M] = & \{ -(t_{ss} + \Delta t_{ss}) \cos(\theta/2) s_M^{\uparrow+} s_{M+1}^{\uparrow+} \\ & -(t_s^F + \Delta t_s^F) s_M^{\uparrow+} s_{M-1}^{\uparrow+} \\ & -(t_{ss} - \Delta t_{ss}) \cos(\theta/2) s_M^{\downarrow+} s_{M+1}^{\downarrow+} \\ & -(t_s^F - \Delta t_s^F) s_M^{\downarrow+} s_{M-1}^{\downarrow+} \\ & -(t_{dd} + \Delta t_{dd}) \cos(\theta/2) d_M^{\uparrow+} d_{M+1}^{\uparrow+} \\ & -(t_d^F + \Delta t_d^F) d_M^{\uparrow+} d_{M-1}^{\uparrow+} \\ & -(t_{dd} - \Delta t_{dd}) \cos(\theta/2) d_M^{\downarrow+} d_{M+1}^{\downarrow+} \\ & -(t_d^F - \Delta t_d^F) d_M^{\downarrow+} d_{M-1}^{\downarrow+} \\ & -(t_{sd} + \Delta t_{sd}) \cos(\theta/2) s_M^{\uparrow+} d_{M+1}^{\uparrow+} \\ & -(t_{sd} - \Delta t_{sd}) \cos(\theta/2) s_M^{\downarrow+} d_{M+1}^{\downarrow+} \\ & -(t_{ds} + \Delta t_{ds}) \cos(\theta/2) d_M^{\uparrow+} s_{M+1}^{\uparrow+} \\ & -(t_{ds} - \Delta t_{ds}) \cos(\theta/2) d_M^{\downarrow+} s_{M+1}^{\downarrow+} \\ & -(\gamma_{ss} + \Delta \gamma_{ss}) \sin(\theta/2) s_M^{\uparrow+} s_{M+1}^{\downarrow+} \\ & -(\gamma_{ss} - \Delta \gamma_{ss}) \sin(\theta/2) s_M^{\downarrow+} s_{M+1}^{\uparrow+} \\ & -(\gamma_{dd} + \Delta \gamma_{dd}) \sin(\theta/2) d_M^{\uparrow+} d_{M+1}^{\downarrow+} \\ & -(\gamma_{dd} - \Delta \gamma_{dd}) \sin(\theta/2) d_M^{\downarrow+} d_{M+1}^{\uparrow+} \\ & -(\gamma_{sd} + \Delta \gamma_{sd}) \sin(\theta/2) s_M^{\uparrow+} d_{M+1}^{\downarrow+} \\ & -(\gamma_{sd} - \Delta \gamma_{sd}) \sin(\theta/2) s_M^{\downarrow+} d_{M+1}^{\uparrow+} \\ & -(\gamma_{ds} + \Delta \gamma_{ds}) \sin(\theta/2) d_M^{\uparrow+} s_{M+1}^{\downarrow+} \\ & -(\gamma_{ds} - \Delta \gamma_{ds}) \sin(\theta/2) d_M^{\downarrow+} s_{M+1}^{\uparrow+} \\ & + \epsilon_{s,F}^{\uparrow} s_M^{\uparrow+} s_M^{\uparrow+} + \epsilon_{s,F}^{\downarrow} s_M^{\downarrow+} s_M^{\downarrow+} + \epsilon_{d,F}^{\uparrow} d_M^{\uparrow+} d_M^{\uparrow+} + \epsilon_{d,F}^{\downarrow} d_M^{\downarrow+} d_M^{\downarrow+} \} \quad (A2) \end{aligned}$$

Schrödinger equation

$$\hat{H}[M]\Psi = E\Psi$$

where Ψ has form (11), results in the following system of equations:

$$\begin{aligned} & -(t_{ss} + \Delta t_{ss}) \cos(\theta/2) f^{\uparrow}(M+1) \\ & -(t_{sd} + \Delta t_{sd}) \cos(\theta/2) g^{\uparrow}(M+1) \\ & -(t_s^F + \Delta t_s^F) f^{\uparrow}(M-1) \\ & -(\gamma_{ss} + \Delta \gamma_{ss}) \sin(\theta/2) f^{\downarrow}(M+1) \\ & -(\gamma_{sd} + \Delta \gamma_{sd}) \sin(\theta/2) g^{\downarrow}(M+1) \\ & + \epsilon_{s,F}^{\uparrow} f^{\uparrow}(M) = E f^{\uparrow}(M) \quad \text{for } s_M^{\uparrow+} |0\rangle \end{aligned} \quad (A3_1)$$

$$\begin{aligned} & -(t_{ss} - \Delta t_{ss}) \cos(\theta/2) f^{\downarrow}(M+1) \\ & -(t_{sd} - \Delta t_{sd}) \cos(\theta/2) g^{\downarrow}(M+1) \\ & -(t_s^F - \Delta t_s^F) f^{\downarrow}(M-1) \\ & -(\gamma_{ss} - \Delta \gamma_{ss}) \sin(\theta/2) f^{\uparrow}(M+1) \\ & -(\gamma_{sd} - \Delta \gamma_{sd}) \sin(\theta/2) g^{\uparrow}(M+1) \\ & + \epsilon_{s,F}^{\downarrow} f^{\downarrow}(M) = E f^{\downarrow}(M) \quad \text{for } s_M^{\downarrow+} |0\rangle \end{aligned} \quad (A3_2)$$

$$\begin{aligned} & -(t_{dd} + \Delta t_{dd}) \cos(\theta/2) g^{\uparrow}(M+1) \\ & -(t_{ds} + \Delta t_{ds}) \cos(\theta/2) f^{\uparrow}(M+1) \\ & -(t_d^F + \Delta t_d^F) g^{\uparrow}(M-1) \\ & -(\gamma_{dd} + \Delta \gamma_{dd}) \sin(\theta/2) g^{\downarrow}(M+1) \\ & -(\gamma_{ds} + \Delta \gamma_{ds}) \sin(\theta/2) f^{\downarrow}(M+1) \\ & + \epsilon_{d,F}^{\uparrow} g^{\uparrow}(M) = E g^{\uparrow}(M) \quad \text{for } d_M^{\uparrow+} |0\rangle \end{aligned} \quad (A3_3)$$

$$\begin{aligned}
& -(t_{dd} - \Delta t_{dd}) \cos(\theta/2) g^\downarrow(M+1) \\
& -(t_{ds} - \Delta t_{ds}) \cos(\theta/2) f^\downarrow(M+1) \\
& -(t_d^F - \Delta t_d^F) g^\downarrow(M-1) \\
& -(v_{dd} - \Delta v_{dd}) \sin(\theta/2) g^\uparrow(M+1) \\
& -(v_{sd} - \Delta v_{sd}) \sin(\theta/2) f^\uparrow(M+1) \\
& + \varepsilon_{d,F}^\downarrow g^\downarrow(M) = E g^\downarrow(M) \quad \text{for } d_M^{\downarrow+} |0\rangle
\end{aligned} \tag{A3_4}$$

These equations lead to the following equations for the wave function coefficients:

$$\begin{aligned}
& -(t_{ss} + \Delta t_{ss}) \cos(\theta/2) \begin{bmatrix} A_B^\uparrow \exp(ik_B^\uparrow b(M+1)) \\ + B_B^\uparrow \exp(-ik_B^\uparrow b(M+1)) \end{bmatrix} \\
& -(t_{sd} + \Delta t_{sd}) \cos(\theta/2) \begin{bmatrix} C_B^\uparrow \exp(ip_B^\uparrow b(M+1)) \\ + D_B^\uparrow \exp(-ip_B^\uparrow b(M+1)) \end{bmatrix} \\
& -(t_s^F + \Delta t_s^F) \begin{bmatrix} A_F^\uparrow \exp(ik_{FM}^\uparrow a(M-1)) \\ + B_F^\uparrow \exp(-ik_{FM}^\uparrow a(M-1)) \end{bmatrix} - \\
& (\gamma_{ss} + \Delta \gamma_{ss}) \sin(\theta/2) \begin{bmatrix} A_B^\downarrow \exp(ik_B^\downarrow b(M+1)) \\ + B_B^\downarrow \exp(-ik_B^\downarrow b(M+1)) \end{bmatrix} - \\
& (\gamma_{sd} + \Delta \gamma_{sd}) \sin(\theta/2) \begin{bmatrix} C_B^\downarrow \exp(ip_B^\downarrow b(M+1)) \\ + D_B^\downarrow \exp(-ip_B^\downarrow b(M+1)) \end{bmatrix} + \\
& \varepsilon_{s,F}^\uparrow \begin{bmatrix} A_F^\uparrow \exp(ik_{FM}^\uparrow aM) \\ + B_F^\uparrow \exp(-ik_{FM}^\uparrow aM) \end{bmatrix} = E \begin{bmatrix} A_F^\uparrow \exp(ik_{FM}^\uparrow aM) \\ + B_F^\uparrow \exp(-ik_{FM}^\uparrow aM) \end{bmatrix}
\end{aligned} \tag{A4_1}$$

$$\begin{aligned}
& -(t_{ss} - \Delta t_{ss}) \cos(\theta/2) \begin{bmatrix} A_B^\downarrow \exp(ik_B^\downarrow b(M+1)) \\ + B_B^\downarrow \exp(-ik_B^\downarrow b(M+1)) \end{bmatrix} \\
& -(t_{sd} - \Delta t_{sd}) \cos(\theta/2) \begin{bmatrix} C_B^\downarrow \exp(ip_B^\downarrow b(M+1)) \\ + D_B^\downarrow \exp(-ip_B^\downarrow b(M+1)) \end{bmatrix} \\
& -(t_s^F - \Delta t_s^F) \begin{bmatrix} A_F^\downarrow \exp(ik_{FM}^\downarrow a(M-1)) \\ + B_F^\downarrow \exp(-ik_{FM}^\downarrow a(M-1)) \end{bmatrix} - \\
& (v_{ss} - \Delta v_{ss}) \sin(\theta/2) \begin{bmatrix} A_B^\uparrow \exp(ip_B^\uparrow b(M+1)) \\ + B_B^\uparrow \exp(-ip_B^\uparrow b(M+1)) \end{bmatrix} \\
& -(v_{sd} - \Delta v_{sd}) \sin(\theta/2) \begin{bmatrix} C_B^\uparrow \exp(ip_B^\uparrow b(M+1)) \\ + D_B^\uparrow \exp(-ip_B^\uparrow b(M+1)) \end{bmatrix} + \\
& \varepsilon_{s,F}^\downarrow \begin{bmatrix} A_F^\downarrow \exp(ik_{FM}^\downarrow aM) \\ + B_F^\downarrow \exp(-ik_{FM}^\downarrow aM) \end{bmatrix} = E \begin{bmatrix} A_F^\downarrow \exp(ik_{FM}^\downarrow aM) \\ + B_F^\downarrow \exp(-ik_{FM}^\downarrow aM) \end{bmatrix}
\end{aligned} \tag{A4_2}$$

$$\begin{aligned}
& -(t_{dd} + \Delta t_{dd}) \cos(\theta/2) \begin{bmatrix} C_B^\uparrow \exp(ip_B^\uparrow b(M+1)) \\ + D_B^\uparrow \exp(-ip_B^\uparrow b(M+1)) \end{bmatrix} \\
& -(t_{ds} + \Delta t_{ds}) \cos(\theta/2) \begin{bmatrix} A_B^\uparrow \exp(ik_B^\uparrow b(M+1)) \\ + B_B^\uparrow \exp(-ik_B^\uparrow b(M+1)) \end{bmatrix} \\
& -(t_d^F + \Delta t_d^F) \begin{bmatrix} C_F^\uparrow \exp(ip_{FM}^\uparrow a(M-1)) \\ + D_F^\uparrow \exp(-ip_{FM}^\uparrow a(M-1)) \end{bmatrix} \\
& -(\gamma_{dd} + \Delta \gamma_{dd}) \sin(\theta/2) \begin{bmatrix} C_B^\downarrow \exp(ip_B^\downarrow b(M+1)) \\ + D_B^\downarrow \exp(-ip_B^\downarrow b(M+1)) \end{bmatrix} \\
& -(\gamma_{sd} + \Delta \gamma_{sd}) \sin(\theta/2) \begin{bmatrix} A_B^\downarrow \exp(ik_B^\downarrow b(M+1)) \\ + B_B^\downarrow \exp(-ik_B^\downarrow b(M+1)) \end{bmatrix} + \\
& \varepsilon_{d,F}^\uparrow \begin{bmatrix} C_F^\uparrow \exp(ip_{FM}^\uparrow aM) \\ + D_F^\uparrow \exp(-ip_{FM}^\uparrow aM) \end{bmatrix} = E \begin{bmatrix} C_F^\uparrow \exp(ip_{FM}^\uparrow aM) \\ + D_F^\uparrow \exp(-ip_{FM}^\uparrow aM) \end{bmatrix}
\end{aligned} \tag{A4_3}$$

$$\begin{aligned}
& -(t_{dd} - \Delta t_{dd}) \cos(\theta/2) \begin{bmatrix} C_B^\downarrow \exp(ip_B^\downarrow b(M+1)) \\ + D_B^\downarrow \exp(-ip_B^\downarrow b(M+1)) \end{bmatrix} \\
& -(t_{ds} - \Delta t_{ds}) \cos(\theta/2) \begin{bmatrix} A_B^\downarrow \exp(ik_B^\downarrow b(M+1)) \\ + B_B^\downarrow \exp(-ik_B^\downarrow b(M+1)) \end{bmatrix} \\
& -(t_d^F - \Delta t_d^F) \begin{bmatrix} C_F^\downarrow \exp(ip_{FM}^\downarrow a(M-1)) \\ + D_F^\downarrow \exp(-ip_{FM}^\downarrow a(M-1)) \end{bmatrix} \\
& -(v_{dd} - \Delta v_{dd}) \sin(\theta/2) \begin{bmatrix} C_B^\uparrow \exp(ip_B^\uparrow b(M+1)) \\ + D_B^\uparrow \exp(-ip_B^\uparrow b(M+1)) \end{bmatrix} \\
& -(v_{sd} - \Delta v_{sd}) \sin(\theta/2) \begin{bmatrix} A_B^\uparrow \exp(ip_B^\uparrow b(M+1)) \\ + B_B^\uparrow \exp(-ip_B^\uparrow b(M+1)) \end{bmatrix} \\
& \varepsilon_{d,F}^\downarrow \begin{bmatrix} C_F^\downarrow \exp(ip_{FM}^\downarrow aM) \\ + D_F^\downarrow \exp(-ip_{FM}^\downarrow aM) \end{bmatrix} = E \begin{bmatrix} C_F^\downarrow \exp(ip_{FM}^\downarrow aM) \\ + D_F^\downarrow \exp(-ip_{FM}^\downarrow aM) \end{bmatrix}
\end{aligned} \tag{A4_4}$$

Similar equations can be written if we start with the basis

$$(s_{M+1}^{\uparrow+} |0\rangle, s_{M+1}^{\downarrow+} |0\rangle, d_{M+1}^{\uparrow+} |0\rangle, d_{M+1}^{\downarrow+} |0\rangle)$$

As a result we obtain eight linear equations which relate to the wave function coefficients in the neighboring layers. Applying this procedure to each interface, we eventually express the wave function coefficients of the first layer through the wave function coefficients of the last layer. Then we impose some boundary conditions (i.e. the values of some coefficients like the amplitude of the incoming wave in the left outer layer and the absence of the reflected waves in the right outer layer) and solve the system of the equations. Therefore, we calculate the wave function of the multilayer.

Acknowledgements

The authors are grateful to Samsung Electronics Co., Ltd. and the Russian Foundation for Basic Research for support. Nomenclature.

References

- [1] T. Valet and A. Fert, "Theory of the perpendicular magnetoresistance in magnetic multilayers", Phys. Rev. B. vol. 48, pp. 7099-7113, September 1993.
- [2] R.Q.Hood, L.M. Falicov, "Boltzmann-equation approach to the negative magnetoresistance of ferromagnetic-normal metal multilayers", Phys. Rev. B, vol. 46, pp. 8287-8298, October 1992.
- [3] J.C. Slonczewski, "Conductance and exchange coupling of two ferromagnets separated by a tunneling barrier", Phys. Rev. B, vol. 39, pp. 6995-7002, April 1989.
- [4] A. Vedyayev, B. Dieny and N. Ryzhanova, "Quantum theory of Giant Magnetoresistance of Spin-Valve Sandwiches", Europhys. Lett., vol. 19, pp. 329-336, June 1992.
- [5] E. Camblong, P. M. Levy and S. Zhang, "Electron transport in magnetic inhomogeneous media", Phys. Rev. B, vol. 51, pp. 16052-16072, June 1995.
- [6] J. Mathon, "Tight-binding theory of tunneling giant magnetoresistance", Phys. Rev. B, vol. 56, pp. 11810-11819, November 1997.
- [7] A. Vedyayev, N. Ryzhanova, C. Lacroix, L. Giacomoni, B.

- Dieny, "Resonance in tunneling through magnetic valve tunnel junctions", *Europhys. Lett.*, vol. 39, pp. 219-224, July 1997.
- [8] J. Mathon, A. Umerski, "Theory of resonant tunneling in epitaxial Fe/AuMgO/Fe(001) junction", *Phys. Rev. B*, vol. 71, 220402(R) (4 pp.), June 2005.
- [9] J.M. MacLaren, X.-G. Zhang, W.H. Butler, X. Wang, "Layer KKR approach to Bloch-wave transmission and reflection: Application to spin-dependent tunneling", *Phys. Rev. B*, vol. 59, pp. 5470-5478, February 1999.
- [10] J. Kudrnovský, V. Drchal, C. Blaas and P. Weinberger, Ab initio theory of perpendicular magnetotransport in metallic multilayers, *Physical Review B*, vol. 62, pp. 15084-15095, December 2000.
- [11] H. Butler, X.-G. Zhang, T.C. Schulthess, J.M. MacLaren, "Spin-dependent tunneling conductance of Fe|MgO|Fe sandwiches", *Phys. Rev. B*, vol. 63, 054416 (12 pp.), February 2001.
- [12] A. Vedyayev, N. Ryzhanova, N. Strelkov, M. Chshiev, and B. Dieny, "A two-band model of spin-polarized transport in Fe/Cr/MgO/Fe magnetic tunnel junctions", *J. Appl. Phys.*, vol. 107, p. 09C720, May 2010.
- [13] E. Y. Tsymbal, O. N. Mryasov, P. R. LeClair, "Spin-dependent tunneling in magnetic tunnel junctions", *J. Phys.: Cond. Matter*, vol. 15, pp. R103-R142, January 2003.
- [14] E.Y. Tsymbal, K.D. Belashchenko, J.P. Velev, S.S. Jaswal, M. van Schilfgaarde, I.I. Oleynik, D.A. Stewart, "Interface effects in spin-dependent tunneling", *Progr. in Mat. Sci.*, vol. 52, pp. 401-420, February-March 2007.
- [15] A.N. Chantis, K.D. Belashchenko, D.L. Smith, E.Y. Tsymbal, M. van Schilfgaarde, and R.C. Albers, "Reversal of Spin Polarization in Fe/GaAs(001) Driven by Resonant Surface States: First-principal Calculations", *Phys. Rev. Lett.*, vol. 99, 196603 (4 pp.), November 2007.
- [16] M.D. Stiles, A. Zangwill, "Anatomy of spin-transfer torque", *Phys. Rev. B* vol. 66, 014407 (14 pp.), July 2002.
- [17] J.C. Slonczewski, Current-driven excitation of magnetic multilayers, *JMMM*, vol. 159, pp. L1-L7, June 1996.
- [18] L. Berger, "Emission of spin wave by a magnetic multilayer traversed by a current", *Phys. Rev. B*, vol. 54, pp. 9353-9358, October 1996.
- [19] A. Shpiro, P.M. Levy, S. Zhang, "Self-consistent treatment of nonequilibrium spin torques in magnetic multilayers", *Phys. Rev. B*, vol. 67, 104430 (17 pp.), March 2003.
- [20] C. Heide, P. E. Zilberman, and J. R. Elliot, Current-driven switching of magnetic layers, *Phys. Rev. B*, vol. 63, 064424 (7 pp.), February 2001.
- [21] A. Manchon, N. Ryzhanova, N. Strelkov, A. Vedyayev, B. Dieny, "Modelling spin transfer torque and magnetoresistance in magnetic multilayers", *J. Phys.: Cond. Matter*, vol. 19, 165212 (42 pp.), April 2007.
- [22] F. Garcia-Moliner F and V.R. Velasco, *Theory of Single and Multiple Interfaces*, World Scientific, Singapore, 1992.
- [23] A. Vedyayev, N. Ryzhanova, R. Vlutters, B. Dieny and N. Strelkov, "Voltage dependence of giant tunnel magnetoresistance in triple barrier magnetic systems", *J. Phys.: Cond. Matter*, vol. 12, pp. 1797-1804, February 2000.
- [24] S. Datta, "Electronic Transport in Mesoscopic Systems", Cambridge University Press, 1997.
- [25] A. Manchon, N. Ryzhanova, A. Vedyayev, M. Chshiev, and B. Dieny, "Description of current-driven torques in magnetic tunnel junctions", *J. Phys.: Cond. Matter*, vol. 20, 145208 (33 pp.), April 2008.
- [26] Xingtao Jia, Ke Xia, Youqi Ke and Hong Guo, "Nonlinear bias dependence of spin-transfer torque from atomic first principles", *Phys. Rev. B*, vol. 84, 014401 (5 pp.), July 2011.
- [27] P. Bruno, "Theory of interlayer magnetic coupling", *Phys. Rev. B*, vol. 52, pp. 411-439, July 1995.